

Superfluidity of liquid 4He confined to one-dimensional straight nanochannel structures

著者 (英)	Junko Taniguchi, Yosuke Aoki, Masaru Suzuki
journal or publication title	Physical Review B
volume	82
number	10
page range	104509
year	2010-09-15
URL	http://id.nii.ac.jp/1438/00009290/

doi: 10.1103/PhysRevB.82.104509

Superfluidity of liquid ^4He confined to one-dimensional straight nanochannel structuresJunko Taniguchi,^{*} Yosuke Aoki, and Masaru Suzuki*Department of Applied Physics and Chemistry, University of Electro-Communications, Chofu, Tokyo 182-8585, Japan*

(Received 17 September 2009; revised manuscript received 12 July 2010; published 15 September 2010)

Superfluidity of liquid ^4He confined in one-dimensional (1D) nanometer-size channels has been studied by means of a torsional oscillator. When the channel is larger than 2.8 nm in diameter, liquid ^4He becomes superfluid at low temperatures and a dissipation due to quantized vortex is observed. The superfluid onset temperature is 1.8 K at 0.14 MPa for the 4.7 nm channel and 0.89 K at 0.01 MPa for the 2.8 nm channel. For the latter, it is suppressed strongly under the application of pressure, and continuously approaches zero at around 2.1 MPa at absolute zero, which suggests a quantum phase transition between the superfluid and nonsuperfluid states in the 1D channel.

DOI: [10.1103/PhysRevB.82.104509](https://doi.org/10.1103/PhysRevB.82.104509)

PACS number(s): 67.25.dj, 61.46.-w, 64.70.Tg, 67.25.dr

I. INTRODUCTION

Liquid ^4He undergoes the superfluid transition due to Bose-Einstein condensation (BEC). It is well known that the confinement of liquid ^4He within porous media suppresses the superfluid onset temperature T_C .¹ Recently it was reported that the superfluidity is strongly suppressed in nanoporous glass, Gelsil, which possesses a three-dimensional (3D) network of 2.5 nm pores. Furthermore, under a certain pressure at absolute zero, the quantum phase transition between the superfluid and nonsuperfluid states takes place.² The suppression of superfluidity in this system is discussed in terms of the separation between the superfluidity and BEC. In the case of 3D random network of pores, it has been found that the localization of BEC (LBEC) takes place at higher temperature than T_C .³⁻⁷

Ultracold atomic gases have been used to study for BEC since its discovery in dilute trapped alkali atoms^{8,9} and have opened a new research field for the Bose system. By controlling the atomic traps, various states of atomic gases have been realized. One interesting state is an atomic gas in a one-dimensional (1D) trap. As the repulsive interaction between bosonic atoms is increased, they are expected to vary from a BEC-type gas to a Tonks-Girardeau gas, which exhibits fermionic properties.^{10,11} In fact, the total energy¹² and the momentum distribution¹³ of the 1D trapped bosonic atoms have been measured and are in good agreement with a theory of the fermionized gas.

It is, therefore, of great importance for several reasons to study the superfluidity and BEC of liquid ^4He confined in a uniform 1D channel: liquid ^4He is remarkably dense compared to ultracold atomic gases, and thus the interparticle interaction is expected to play a significant role in the superfluidity and BEC. It is also interesting to compare liquid ^4He confined in the 1D channel with that in 3D random network of pores. In this paper, we report the superfluidity of liquid ^4He confined in 1D nanometer-size channels of folded sheets mesoporous materials (FSM). FSM are a family of highly ordered porous silica crystals with regular arrangement of uniform hexagonal channels with no connection between themselves.¹⁴ Down to a 2.8 nm sample, the superfluid and the quantized vortex were confirmed. Furthermore, we found that the superfluid for the 2.8 nm sample was strongly suppressed by pressurization.

II. EXPERIMENTAL

The superfluidity of liquid ^4He was measured by a torsional oscillator. We prepared three kinds of FSM powders, of which the 1D channel was 2.2, 2.8, and 4.7 nm in diameter and 0.2–0.5 μm in length. FSM powder was mixed with 70 μm silver powder in a two-to-one mass ratio, pressed onto a Be-Cu cap of torsional oscillator (OD12.0 mm \times h4.0 mm), and then sintered at 200 $^\circ\text{C}$ under 500 kgf/cm² to avoid powder crushing. Before the cap was epoxyed to the torsion head, the top surface of the pellet was filed to adjust the side wall of the cap, in order to minimize the interspace between the pellet and the inner wall of the torsion head. The final dimension of the pellet is ϕ 10.0 mm \times t2.5 mm.

The torsional oscillator consists of a Be-Cu head containing the pellet and a Be-Cu hollow torsion rod. The torsion head oscillates at a resonance frequency of 2.06 kHz with a high-quality factor of $Q=1.3 \times 10^6$ in a vacuum at 4 K. The rim velocity of torsional oscillator is less than 3 mm/s, in the present experiments.

We here describe the experimental details for the 2.8 nm sample. By fitting the N_2 adsorption isotherm at 77 K, the total surface area of the pellet was found to be 114 m² while the outer surface area of powders was estimated to be 12 m² from the t-plot method.¹⁵ The porosity in the 1D channel of FSM was $44 \pm 2\%$, and the volume of outside powders was $18 \pm 2\%$ of the apparent volume of the pellet. About 70% of ^4He atoms in the channel remain inert solid under the saturated vapor pressure (SVP),¹⁶ and the effective diameter of liquid ^4He is estimated as about 1.5 nm. For torsional oscillator measurements of liquid, the resonance frequency increased below the bulk superfluid transition, T_λ , because of the volume of outside powders, but the ratio of this contribution was not large compared with liquid ^4He in the 1D channel.

III. RESULTS

The torsional oscillator measurements were performed for 2.2, 2.8, and 4.7 nm samples from 2.5 down to 0.15 K. Figure 1(a) shows the change in resonance frequency from T_λ for those samples filled with liquid ^4He under low pres-

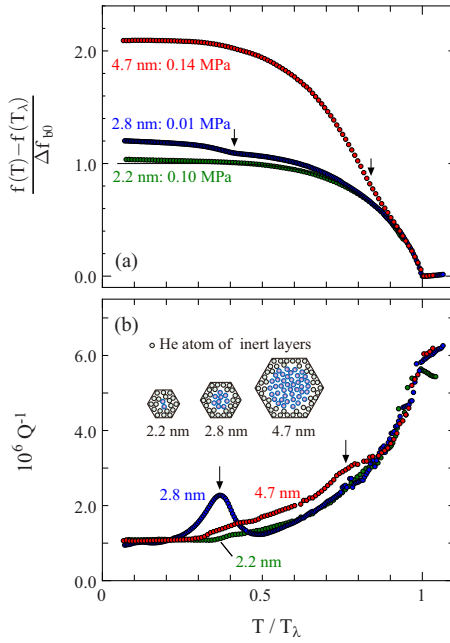


FIG. 1. (Color online) (a) Change in the resonance frequency from T_λ for 2.2, 2.8, and 4.7 nm samples filled with liquid ^4He under low pressure. The abscissa is the normalized temperature divided by T_λ and the frequency change in the ordinate is divided by the contribution of superfluid outside powders at absolute zero. Solid curve is the contribution of bulk superfluid. Arrows denote T_C in the channel. (b) Change in Q^{-1} . Arrows denote T_{peak} . Inset: schematic sectional view of the channels filled with ^4He .

sure. The abscissa is the normalized temperature divided by T_λ , and the frequency change in the ordinate is divided by the contribution of superfluid outside powders at absolute zero, Δf_{b0} . The contribution of superfluid outside powders is shown as a solid curve in the figure. As seen, the sets of data fall on the universal curve above $T/T_\lambda = 0.92$ (2.0 K) and deviate from the curve. For the 2.2 nm sample, although there is a slight deviation from the curve at low temperatures, no rapid increase is observed.¹⁷ On the contrary, a clear rapid increase is observed for the 2.8 nm sample at $T/T_\lambda = 0.41$ (0.89 K) and for the 4.7 nm sample at $T/T_\lambda = 0.84$ (1.80 K). This rapid increase can be attributed to decoupling from the oscillation due to the superfluid in the 1D channel.

The decoupling of superfluid in the channel was found to depend strongly on the channel diameter. For the 4.7 nm sample, the ratio between the decoupled superfluid and the total liquid in the channel, D_{in} is $\sim 30\%$ at the lowest temperature. It agrees with the ratio defined in the same way for ^4He outside powder, D_{out} . On the contrary, for 2.8 nm sample, D_{in} is small as $\sim 10\%$, compared with $D_{\text{out}} \sim 30\%$.

Change in the Q factor is shown as a function of normalized temperature in Fig. 1(b). As the temperature is decreased, Q^{-1} for all samples has a break at T_λ . For the 2.2 nm sample, Q^{-1} decreases monotonously below this break. In contrast, Q^{-1} for the 2.8 nm sample has a significantly large peak at $T/T_\lambda = 0.37$ (0.80 K). In addition, Q^{-1} for the 4.7 nm sample also has a peak at $T/T_\lambda \cong 0.76$ (1.62 K), which is more ambiguous and broader than that for the 2.8 nm

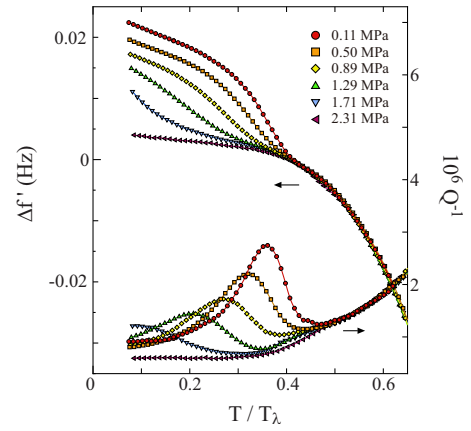


FIG. 2. (Color online) Change in the resonance frequency and Q^{-1} for the 2.8 nm sample under various pressures. The frequency change $\Delta f'$ in the ordinate is corrected by multiplication of the density ratio, $\{\rho(0.1 \text{ MPa})\}/\rho(P)$, and is shifted to fall on the universal curve.

sample. For both, the peak temperature, T_{peak} , is located below the temperature where the resonance frequency exhibits a rapid increase.

Figure 2 shows the change in the resonance frequency and Q factor for the 2.8 nm sample under pressures. The abscissa is the normalized temperature divided by T_λ of each pressure while the frequency change $\Delta f'$ in the ordinate is corrected by multiplication of the density ratio, $\{\rho(0.1 \text{ MPa})\}/\rho(P)$, and is shifted to fall on the universal curve. Above around $T/T_\lambda = 0.4$, all sets of data are in good agreement with each other and below this temperature they separate depending on pressure. For 0.11 MPa, a rapid increase in $\Delta f'$ is observed at $T/T_\lambda = 0.41$. As the pressure is increased, the increase in $\Delta f'$ shifts to lower temperature and its magnitude becomes small. As the pressure is increased further, no increase is observed above 2.3 MPa. The observed increase in $\Delta f'$ is accompanied by a dissipation. At high temperatures, Q^{-1} for all pressures falls on the universal curve which decreases with decreasing temperature. For 0.11 MPa, Q^{-1} starts to increase at around $T/T_\lambda = 0.5$ and takes a maximum value at $T/T_\lambda = 0.36$. T_{peak} shifts to a lower temperature by pressurization, accompanied by a decrease in peak height. Above 2.3 MPa, no additional increase in Q^{-1} is observed.

It is important to note that T_{peak} coincides with the temperature at the steepest slope of the increase in $\Delta f'$, and that T_{peak} shifts to a lower temperature by pressurization. This suggests that the superfluid in the channel grows around T_{peak} as the temperature is decreased. Thus, we can conclude that the superfluid onset in the 1D channel takes place slightly above T_{peak} . Here, we define T_C in the channel from the resonance frequency as the intersection of the extrapolation from high temperatures and the steepest increase.

The dissipation below T_C is an evidence in the existence of the superfluid in the 1D channel. The fluctuation of the phase coherence of superfluid becomes large at around T_C , which may cause the phase slip by the expansion of quantized vortex in the channel. We here apply the competing barrier model of quantized vortex,¹⁸ in which the vortex expands to the channel across the superfluid flow by the ther-

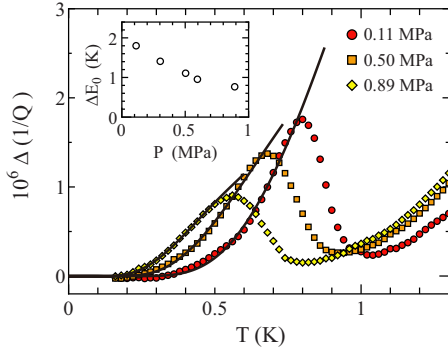


FIG. 3. (Color online) $\Delta(1/Q)$ as a function of temperature. Solid curves are calculated from Eq. (2) with the fitting parameters ΔE_0 and $2\kappa\nu Wp_c$. Inset: $\Delta E_0/k_B$ as a function of pressure.

mal activation process to overcome the barrier energy ΔE . In the 1D channel the superfluid flows in the axis direction, and the barrier energy ΔE is shifted by the superfluid flow as $\Delta E = \Delta E_0 \pm p_c v_s$, where ΔE_0 is the barrier energy of no superflow, p_c is the impulse of the vortex, and v_s is the superfluid velocity. The double sign depends on the mutual direction between the impulse and the superfluid flow. Thus, the decay of superfluid velocity is expressed as

$$\frac{dv_s}{dt} = -2\kappa\nu N_v \exp\left(-\frac{\Delta E_0}{k_B T}\right) \sinh\left(\frac{p_c v_s}{k_B T}\right). \quad (1)$$

Here, $\kappa = 0.998 \times 10^{-3} \text{ cm}^2/\text{s}$ is the circulation quantum, ν is the attempt frequency for the expansion, and N_v is the number of vortices per unit length.

In a nanometer-size channel, we can expect that the vortex is thermally created. The number of vortices is obtained as $N_v = W \exp(-\Delta E'/k_B T)$, where W is the number of nucleation sites per unit length and $\Delta E'$ is the thermal activation energy for vortex creation.¹⁹ When the channel is nanometer size, $\Delta E'$ would be much the same as ΔE_0 . The persistent current described in Eq. (1) decays exponentially under a condition where the superfluid velocity is small enough, and this decay is related to the dissipation, i.e., the decrease in Q factor. Assuming that $\Delta E' = \Delta E_0$, we finally obtain

$$\Delta\left(\frac{1}{Q}\right) = \frac{2\kappa\nu W p_c}{k_B T \omega_R} \exp\left(-\frac{2\Delta E_0}{k_B T}\right), \quad (2)$$

where ω_R is the resonance angular frequency of the torsional oscillator. $\Delta(1/Q)$ increases rapidly as the temperature is increased. Figure 3 shows the comparison between the experimental data of the 2.8 nm sample and fitted curves with the parameters of the barrier energy ΔE_0 and a factor of $2\kappa\nu W p_c$ in Eq. (2).²⁰ The obtained value of the fitting parameter, ΔE_0 , is plotted against pressure in the inset of Fig. 3. It is not so far from the estimated value of $\Delta E'$.¹⁹ We can conclude that the dissipation is well explained by the presence of quantized vortices in the channel.

Figures 4(a) and 4(b) show T_C and T_{peak} for 2.8 and 4.7 nm samples under pressure, associated with the superfluid onset and dissipation peak temperatures of unsaturated ^4He films in Fig. 4(b). T_C for the 4.7 nm sample is 1.8 K at 0.14 MPa. It is suppressed weakly with increasing pressure and

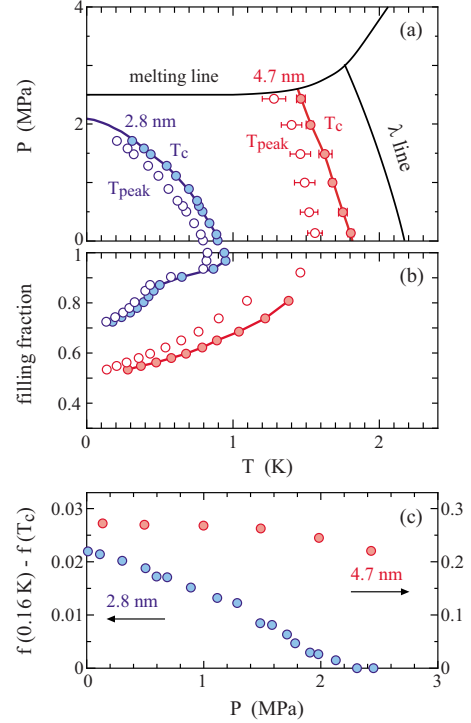


FIG. 4. (Color online) (a) T_C and T_{peak} for the 2.8 and 4.7 nm samples under pressure. (b) Superfluid onset and dissipation peak temperatures of unsaturated ^4He films. The ordinate is the filling fraction of the channel. (c) Increase in the resonance frequency from T_C as a function of pressure.

terminates at the melting pressure. The dissipation peak for this sample is also observed at T_{peak} which is slightly below T_C . Its height is quite low and is comparable with that of the 2.8 nm sample. On the other hand, T_C for the 2.8 nm sample is much lower than that of the 4.7 nm one and is 0.90 K at 0.01 MPa. Furthermore, it is suppressed strongly by pressurization and tends to absolute zero at around 2.1 MPa below the melting pressure of bulk liquid. It was found that T_C and T_{peak} of both samples are smoothly connected with the superfluid onset and dissipation peak temperatures of unsaturated ^4He films.

The increase in the frequency at the lowest temperature from T_C is plotted as a function of pressure in Fig. 4(c). For the 4.7 nm sample, the increase is almost constant at low pressure, and then decreases slightly with increasing pressure above about 1.5 MPa. On the other hand, increase for the 2.8 nm sample decreases almost linearly with increasing pressure and continuously approaches zero at around 2.1 MPa.

IV. DISCUSSION

We compare the present experiments with those of 3D nanoporous media, Vycor glass and Gelsil. Typical diameter of these pores are 6 nm for Vycor glass and 2.5 nm for Gelsil, respectively. T_C for Vycor glass is shifted to 1.94 K at SVP and decreases almost in parallel with the λ line.²¹ On the other hand, T_C for Gelsil is 1.4 K at SVP and is suppressed strongly by pressurization. It reaches absolute zero at

3.5 MPa which is below the melting pressure in Gelsil, indicating a quantum phase transition from the superfluid to non-superfluid states.⁴

T_C in the 1D channel shows a similar behavior. For a large 1D channel, T_C decreases almost in parallel with the λ line. When the channel diameter narrows, it is suppressed strongly by pressurization. T_C for the 2.8 nm sample under pressure tends to absolute zero at around 2.1 MPa. This indicates that a quantum phase transition between the superfluid and non-superfluid states takes place in the 1D channel. The extreme confinement induces the transition in spite of the dimensionality in the connection of nanopores. Here, we should note a significant difference. A large dissipation peak was observed below T_C for the present experiments while no dissipation for Gelsil.²²

The mechanism for the suppression of superfluidity in the 1D channel is an interesting subject. For 3D nanoporous media, the suppression has been discussed in terms of LBEC. On the contrary, the potential in the 1D channel for confinement is uniform in the axis direction. Whether the separation of superfluid transition and BEC is caused even without 3D random network is a subject for future study. Heat-capacity study of ^4He in the 1D channel or to compare systematically the size dependence of superfluid suppression between 3D nanoporous media and 1D channel will be meaningful.

Here we note the dimensionality of liquid ^4He in 2.8 nm channel. Comparison between diameter of the channel and the thermal de Broglie wavelength of ^4He atom $\Lambda = h/\sqrt{2\pi mk_B T}$ is frequently used to discuss the reduction of dimensionality for a free particle system. The wavelength is 0.9 nm at 1 K and reaches 2.8 nm at 0.1 K. Then, the liquid ^4He atom in the channel of the 2.8 nm sample is a quasi-one-dimensional system, at least at low temperatures. Regarding the superfluidity, the dimensionality has been discussed in terms of the coherence length. The superfluid ^4He film is regarded as two dimensional, since the film thickness is smaller than the coherence length ~ 0.3 nm.²³ In the case of 2.8 nm channel, as mentioned above, the effective diameter

of liquid ^4He is estimated as about 1.5 nm, which is larger than the coherence length of bulk superfluid. However, the strong suppression of superfluidity by the application of pressure is not necessarily understood by the simple size effect of 3D superfluid transition.

In the case of bulk liquid ^4He , it is argued that the application of pressure inhibits particle exchange and decreases T_λ .²⁴ In the 1D Bose system, it is well recognized that the degree of particle exchange determines physical properties.^{10,11} The suppression of T_C in the present experiments may be related to the inhibition of particle exchange in the channel.

V. SUMMARY

We measured the superfluidity of liquid ^4He confined in 1D nanometer-size channels of 2.2, 2.8, and 4.7 nm in diameter. Down to the 2.8 nm sample, the superfluid in the 1D channel was clearly observed at low temperatures, and a dissipation due to quantized vortex is confirmed. While T_C for the 4.7 nm sample decreases almost parallel to the λ line with increasing pressure, T_C for the 2.8 nm sample is strongly suppressed and continuously approaches zero at around 2.1 MPa. This behavior of this sample indicates a quantum phase transition between the superfluid and non-superfluid states. It is of importance to clarify whether the suppression of the superfluidity in the 1D channel is the same mechanism as that of 3D nanoporous media. This is a subject for future study.

ACKNOWLEDGMENTS

We thank S. Inagaki for the supply of FSM. This work was partly supported by a Grant-in-Aid for Scientific Research on Priority Areas ‘‘Physics of Super-clean Materials’’ from the Ministry of Education, Culture, Sports, Science and Technology (MEXT).

*tany@phys.uec.ac.jp

¹J. R. Beamish, A. Hikata, L. Tell, and C. Elbaum, *Phys. Rev. Lett.* **50**, 425 (1983).

²K. Yamamoto, H. Nakashima, Y. Shibayama, and K. Shirahama, *Phys. Rev. Lett.* **93**, 075302 (2004).

³K. Yamamoto, Y. Shibayama, and K. Shirahama, *Phys. Rev. Lett.* **100**, 195301 (2008).

⁴K. Yamamoto, Y. Shibayama, and K. Shirahama, *J. Phys. Soc. Jpn.* **77**, 013601 (2008).

⁵O. Plantevin, H. R. Glyde, B. Fak, J. Bossy, F. Albergamo, N. Mulders, and H. Schober, *Phys. Rev. B* **65**, 224505 (2002).

⁶A. V. Lopatin and V. M. Vinokur, *Phys. Rev. Lett.* **88**, 235503 (2002).

⁷M. Kobayashi and M. Tsubota, [arXiv:cond-mat/0510335](https://arxiv.org/abs/cond-mat/0510335) (unpublished); *Low Temperature Physics: 24th International Conference on Low Temperature Physics, LT24*, AIP Conf. Proc. No. 850 (AIP, New York, 2006), p. 287.

⁸M. H. Anderson, J. R. Ensher, M. R. Matthews, C. E. Wieman, and E. A. Cornell, *Science* **269**, 198 (1995).

⁹K. B. Davis, M. O. Mewes, M. R. Andrews, N. J. van Druten, D. S. Durfee, D. M. Kurn, and W. Ketterle, *Phys. Rev. Lett.* **75**, 3969 (1995).

¹⁰L. Tonks, *Phys. Rev.* **50**, 955 (1936).

¹¹E. H. Lieb and W. Liniger, *Phys. Rev.* **130**, 1605 (1963).

¹²T. Kinoshita, T. Wenger, and D. Weiss, *Science* **305**, 1125 (2004).

¹³B. Paredes, A. Widera, V. Murg, O. Mandel, S. Fölling, I. Cirac, G. V. Shlyapnikov, T. W. Mänsch, and I. Bloch, *Nature (London)* **429**, 277 (2004).

¹⁴S. Inagaki, A. Koiwai, N. Suzuki, Y. Fukushima, and K. Kuroda, *Bull. Chem. Soc. Jpn.* **69**, 1449 (1996); S. Inagaki, Y. Fukushima, and K. Kuroda, *J. Chem. Soc., Chem. Commun.* **22**, 680 (1993).

¹⁵B. C. Lippens and J. H. de Boer, *J. Catal.* **4**, 319 (1965).

- ¹⁶H. Ikegami, Y. Yamato, T. Okuno, J. Taniguchi, N. Wada, S. Inagaki, and Y. Fukushima, *Phys. Rev. B* **76**, 144503 (2007).
- ¹⁷J. Taniguchi and M. Suzuki, *J. Low Temp. Phys.* **150**, 347 (2008).
- ¹⁸R. J. Donnelly, R. N. Hills, and P. H. Roberts, *Phys. Rev. Lett.* **42**, 725 (1979).
- ¹⁹The kinetic energy of the circulating superfluid for a straight vortex in a cylinder with height ℓ and diameter d is written as $E = \rho_s \kappa^2 \ell \log(d/2a)/4\pi$, where ρ_s is the superfluid density and a is the radius of vortex core. From this equation, we may estimate the activation energy for vortex creation $\Delta E'$ in the channel. When we substitute $d=1.0$ nm, $\ell=1.0$ nm, and $a=0.13$ nm, then $\Delta E'/k_B=11$ K. This value would not be very large for the present experiments.
- ²⁰The second fitting parameter, $2\kappa\nu W p_c$, is the value related to the number of vortices in the channel. The value obtained from fitting for 0.11 MPa is on the order of 1 K/s. Taking into account $\rho_s=0.14$ g/cm³ (density for bulk liquid ^4He at around 0 MPa) and $d=1.0$ nm (the order of channel diameter), $p_c=\rho_s\kappa d^2=1.4 \times 10^{-23}$ kg m s⁻¹, and then, $W\nu=8 \times 10^6$ m⁻¹ s⁻¹. It is difficult to estimate W and ν exactly and separately. If we adopt an idea that one vortex can be created per d , W is estimated as $W=1 \times 10^9$ m⁻¹. When we substitute $\Delta E' = 1.8$ K at 0.11 MPa and $W=1 \times 10^9$ m⁻¹, the number of vortices is 8% of W at 0.7 K, and 23 per one 1D channel 0.3 μm in length. It seems to be enough to break the superflow along the 1D channel. However, it leads to significantly small ν as 8×10^{-3} s⁻¹. The results indicate that the small magnitude of ν in this model is essential, whose origin is an issue in the future.
- ²¹Cao Lie-zhao, D. F. Brewer, C. Girit, E. N. Smith, and J. D. Reppy, *Phys. Rev. B* **33**, 106 (1986).
- ²²K. Shirahama (private communication).
- ²³A. Singasaas and G. Ahlers, *Phys. Rev. B* **30**, 5103 (1984).
- ²⁴G. Chapline, Jr., *Phys. Rev. A* **3**, 1671 (1971).